NASA/TM—2003-212551 AIAA–2003–5278

Performance Evaluation of the NEXT Ion Engine

George C. Soulas, Matthew T. Domonkos, and Michael J. Patterson
Glenn Research Center, Cleveland, Ohio

October 2003

The NASA STI Program Office . . . in Profile

Since its founding, NASA has been dedicated to the advancement of aeronautics and space science. The NASA Scientific and Technical Information (STI) Program Office plays a key part in helping NASA maintain this important role.

The NASA STI Program Office is operated by Langley Research Center, the Lead Center for NASA's scientific and technical information. The NASA STI Program Office provides access to the NASA STI Database, the largest collection of aeronautical and space science STI in the world. The Program Office is also NASA's institutional mechanism for disseminating the results of its research and development activities. These results are published by NASA in the NASA STI Report Series, which includes the following report types:

- TECHNICAL PUBLICATION. Reports of completed research or a major significant phase of research that present the results of NASA programs and include extensive data or theoretical analysis. Includes compilations of significant scientific and technical data and information deemed to be of continuing reference value. NASA's counterpart of peer-reviewed formal professional papers but has less stringent limitations on manuscript length and extent of graphic presentations.

- TECHNICAL MEMORANDUM. Scientific and technical findings that are preliminary or of specialized interest, e.g., quick release reports, working papers, and bibliographies that contain minimal annotation. Does not contain extensive analysis.

- CONTRACTOR REPORT. Scientific and technical findings by NASA-sponsored contractors and grantees.

- CONFERENCE PUBLICATION. Collected papers from scientific and technical conferences, symposia, seminars, or other meetings sponsored or cosponsored by NASA.

- SPECIAL PUBLICATION. Scientific, technical, or historical information from NASA programs, projects, and missions, often concerned with subjects having substantial public interest.

- TECHNICAL TRANSLATION. English-language translations of foreign scientific and technical material pertinent to NASA's mission.

Specialized services that complement the STI Program Office's diverse offerings include creating custom thesauri, building customized databases, organizing and publishing research results . . . even providing videos.

For more information about the NASA STI Program Office, see the following:

- Access the NASA STI Program Home Page at ***http://www.sti.nasa.gov***

- E-mail your question via the Internet to help@sti.nasa.gov

- Fax your question to the NASA Access Help Desk at 301–621–0134

- Telephone the NASA Access Help Desk at 301–621–0390

- Write to:
  NASA Access Help Desk
  NASA Center for AeroSpace Information
  7121 Standard Drive
  Hanover, MD 21076

NASA/TM—2003-212551 AIAA–2003–5278

Performance Evaluation of the NEXT Ion Engine

George C. Soulas, Matthew T. Domonkos, and Michael J. Patterson
Glenn Research Center, Cleveland, Ohio

Prepared for the
39th Joint Propulsion Conference and Exhibit
cosponsored by the AIAA, ASME, SAE, and ASEE
Huntsville, Alabama, July 20–23, 2003

National Aeronautics and
Space Administration

Glenn Research Center

October 2003

This report contains preliminary findings, subject to revision as analysis proceeds.

Available from

NASA Center for Aerospace Information
7121 Standard Drive
Hanover, MD 21076

National Technical Information Service
5285 Port Royal Road
Springfield, VA 22100

Available electronically at http://gltrs.grc.nasa.gov

PERFORMANCE EVALUATION OF THE NEXT ION ENGINE

George C. Soulas, Matthew T. Domonkos, and Michael J. Patterson
National Aeronautics and Space Administration
Glenn Research Center
Cleveland, Ohio

The performance test results of three NEXT ion engines are presented. These ion engines exhibited peak specific impulse and thrust efficiency ranges of 4060–4090 s and 0.68–0.69, respectively, at the full power point of the NEXT throttle table. The performance of the ion engines satisfied all project requirements. Beam flatness parameters were significantly improved over the NSTAR ion engine, which is expected to improve accelerator grid service life. The results of engine inlet pressure and temperature measurements are also presented. Maximum main plenum, cathode, and neutralizer pressures were 12,000 Pa, 3110 Pa, and 8540 Pa, respectively, at the full power point of the NEXT throttle table. Main plenum and cathode inlet pressures required about 6 hours to increase to steady-state, while the neutralizer required only about 0.5 hour. Steady-state engine operating temperature ranges throughout the power throttling range examined were 179–303 °C for the discharge chamber magnet rings and 132–213 °C for the ion optics mounting ring.

Introduction

The success of the NASA Solar Electric Propulsion Technology Applications Readiness (NSTAR) program's ion propulsion system on the Deep-Space 1 spacecraft has secured the future for ion propulsion technology for other NASA missions.[1] While the 2.3 kW NSTAR ion engine input power and service life capabilities are appropriate for Discovery Class as well as other, smaller NASA missions, the application of NSTAR hardware to large flagship-type missions such as outer planet explorers and sample return missions is limited due its lack of power and total impulse capabilities.

As a result, NASA's Office of Space Science awarded a research project to a NASA Glenn Research Center (GRC)-led team to develop the next generation ion propulsion system.[2,3] The propulsion system, called NASA's Evolutionary Xenon Thruster (NEXT), is being developed by a team composed of GRC, the Jet Propulsion Laboratory, Aerojet, Boeing Electron Dynamic Devices, Applied Physics Laboratory, University of Michigan, and Colorado State University.

The NEXT propulsion system will consist of a 40 cm diameter ion engine, a lightweight, modular power processing unit with an efficiency and a specific power equal-to or better-than the NSTAR power processor, and a xenon feed system which uses proportional valves and thermal throttles to significantly reduce mass and volume relative to the NSTAR feed system.

Each component of the propulsion system is required to achieve certain minimum performance, service life, and specific mass requirements. Performance requirements for the NEXT ion engine include a specific impulse of at least 4050 s at full power, and thruster efficiencies of greater than 0.63 and 0.42 at full and low power, respectively. The NEXT ion engine must further provide a 270 kg propellant throughput capability, which ultimately results in a 405 kg qualification throughput requirement.

The NEXT propellant management system is required to deliver xenon flows to the ion engine with an uncertainty of ± 3%. Providing xenon flow throughout the entire throttled flow range with this tight tolerance requires knowledge of engine inlet pressures during operation.

This paper presents the performance test results of three NEXT ion engines. This paper also reports on the results of engine inlet pressure measurements, along with engine temperature measurements. The pressure measurements will be used for the development of the NEXT propellant management system. Results for both investigations were obtained over a thruster input power range of 1.1–6.9 kW.

Test Hardware and Operating Procedures

Ion Engines

The performance of three NEXT ion engines was evaluated. One engine, designated LM2, is a laboratory model engine and is shown in Fig. 1. The other two,

designated EM1 and EM2, are engineering model engines, one of which is shown in Fig. 2. All engines utilize a 40 cm beam extraction diameter, which is double the area of the NSTAR ion engine. The technical approach here is a continuation of the "derating" philosophy used for the NSTAR ion engine. Doubling the beam area allows operation at significantly higher thruster input power while maintaining low voltages and ion current densities. Thus, potential complications associated with high-voltage electrode operations are avoided, and engine longevity can be maintained.

The discharge chamber designs of LM2, EM1, and EM2 utilize a hollow cathode electron emitter and a semi-conic chamber with a ring cusp magnetic circuit for electron containment created by high strength, rare earth magnets. A flake-retention scheme is employed in both discharge chambers, which also acts as a magnet retainer. The material, preparation, and installation processes employed for the flake-retention system are identical to those implemented on the NSTAR engine.[4] The NEXT ion engines also incorporate a reverse-feed propellant injection process for the main plenum.

These ion engines utilized the same neutralizer design, which is mechanically similar to the Hollow Cathode Assembly of the International Space Station Plasma Contactor.[5] Because the neutralizer cathode emission current range on the NEXT ion engine is similar to that of the Hollow Cathode Assembly, the NEXT neutralizer design can leverage off of the large cathode database already available with this design for risk reduction.[6]

Differences between the laboratory model engine (i.e. LM2) and the engineering model engines (i.e. EM1and EM2) included the mechanical fidelity of the hardware, the design of the propellant isolators, and the design of the ion optics' geometry. The mechanical integrity of the EM1 and EM2 engines was designed for the anticipated vibration environment whereas LM2 was not. Engines EM1 and EM2 also utilized new compact propellant isolators with a higher voltage isolation capability of about 1800 V.

All engines utilized the same ion optics assemblies, except for the geometry of the perforated region of the beam extraction electrodes. Engine LM2 utilized the same geometry as employed with the NSTAR engine while those of EM1 and EM2 were similar except that the accelerator electrode thickness was increased to enhance engine service life. The performance of these two electrode geometries is described in detail in Ref. 7.

During one test series, engine EM1 was outfitted with several Type K thermocouples for operating temperature measurements. The locations of several of these thermocouples are indicated in Fig. 3.

Power Console and Gas Feed System

A power console similar to that described in Ref. 8 powered these ion engines. This power console allows for ion engine input powers of over 10 kW with beam power supply voltages of up to 2000 V.

A high purity gas feed system was used to provide xenon to the discharge cathode, main plenum, and neutralizer through separate mass flow controllers. For one test with engine EM1, ion engine inlet pressures for all three propellant lines were measured. This was accomplished with pressure taps at the propellant line inlets to the engine. Pressures were measured with a 1.3×10^4 Pa (100 Torr) capacitance manometer.

Diagnostics

During thruster operation, voltages and currents were measured with digital multimeters and xenon flows with mass flow meters. These measured parameters were used to set engine operating conditions, as well as to determine engine performance.

The engine was connected to an electrically floating power supply circuit used to determine the screen grid transparency to discharge chamber ions. The circuit electrically tied the screen grid to the discharge cathode during normal operation, but biased the grid negative relative to discharge cathode potential to repel electrons and measure the collected ion current.

For performance testing, beam current density profiles were measured with a probe mounted onto a two-axis probe motion system. The probe was a planar geometry with a 1 cm^2 circular current-collecting area. The probe was biased negative with respect to beam plasma potential to repel electrons and was grounded through a resistor that acted as a shunt to measure collected currents.

The positioning system swept the probe in the radial and axial directions through the vertical center of the engine ion optics. The positioning system had a 1.5 m maximum travel in each axis, which enabled near-field radial beam current density measurements at different axial locations, as measured from the geometric center of the ion optics. The current density measurements were then used to determine radial beam current density profiles.

Vacuum Facilities

For the results presented in this paper, testing was conducted in two facilities. The first facility was Vacuum Facility 6 (VF6) at NASA GRC. This 7.6 m diameter × 22.9 m long facility was evacuated with 12 cryogenic pumps and a turbomolecular pump. The total measured facility pumping speed was approximately 227,000 l/s with xenon. The facility base pressure for these tests was typically less than 1.3×10^{-4} Pa (1×10^{-6} Torr). Facility background pressures during testing were 3.2×10^{-4} Pa (2.4×10^{-6} Torr) to 6.0×10^{-4} Pa (4.5×10^{-6} Torr) as measured by an ion gage mounted near the center of the cylindrical section of the facility.

The second facility was Vacuum Facility 11 (VF11) at NASA GRC. This 2.2 m diameter × 7.9 m long facility was evacuated with seven cryogenic pumps and a turbomolecular pump. The total measured facility pumping speed was greater than 100,000 l/s with xenon. The facility base pressure for these tests was typically about 4×10^{-5} Pa (3×10^{-7} Torr).

Facility background pressures in VF11 were less than 9.3×10^{-4} Pa (7×10^{-6} Torr), except at the highest beam current. During operation at the highest beam current, the high xenon flow rates and beam power tended to warm-up three of the seven cryogenic pumps. This reduced the facility's effective pumping speed, and resulted in background pressures that increased with operating time up to 1.6×10^{-3} Pa (1.2×10^{-5} Torr).

Operating Procedures

During each engine test, the engine was operated at a range of engine input powers from 1.1 kW to 6.9 kW. Ion engine beam voltages, accelerator voltages, beam currents, discharge chamber xenon flows, and neutralizer current at these various input power levels are listed in Tables 1 and 2. Table 1 is the NEXT throttle table while Table 2 includes a higher beam current utilized for the NEXT 2000 hour wear test.[9] Main plenum and discharge cathode flow splits were selected to yield discharge voltages of 23–27 V throughout the throttle table, while discharge currents were continually adjusted to maintain a constant beam current.

For the performance results presented in this paper, engines LM2 and EM1 were performance tested in VF6 while engine EM2 was performance tested in VF11. At each operating condition, steady-state operating parameters that included beam power supply, accelerator, discharge, and neutralizer currents and voltages, coupling voltages (i.e. neutralizer cathode voltage relative to tank ground), and xenon flows were measured. Radial beam current density profiles were also measured at several operating points. In addition, ion optics performance parameters such as impingement-limited total voltages, electron backstreaming limits, and screen grid ion transparencies were determined at each operating condition.

For the propellant line inlet pressure and engine temperature measurements, engine EM1 was tested in VF11. During this test, the engine was operated at low and high input power levels. Furthermore, no attempt was made to simulate the thermal environment anticipated for the NEXT engine, so that the engine was allowed to radiate heat to the facility walls and surrounding cryogenic pumps. Engine pressure and temperature increases with time from engine startup were monitored to determine pressure and temperature transients during engine warm-up and steady-state values. To preclude warming-up the cryogenic pumps of VF11, the engine was operated initially without beam extraction until near-steady state conditions were achieved. Then the engine was operated with beam extraction and its effect evaluated. Propellant line inlet pressures with cold gas flow (i.e. without the engine operating) were also measured.

Results and Discussions

Performance Test Results

Overall Engine Performance

The results of performance tests with NEXT engines LM2, EM1, and EM2 are listed in Tables 3, 4, and 5, respectively. The performance test results for EM1 presented herein are the pretest performance results in Ref. 9. The beam divergence thrust correction factor for thrust calculations and the total doubly-to-singly-charged ion current ratio were assumed to be about 0.98 and 0.034–0.044, respectively, based on Ref. 10. Ingested mass flow due to the facility background gas pressure was included in the total mass flow rate to the engine for determining thrust efficiency and specific impulse.[11]

The demonstrated throttling range of all engines was 1.1–6.9 kW. All three engines performed similarly, with thrust efficiencies, thrusts, and specific impulses within about 2% of each other.

The thrusts of all three engines were calculated to be about 50 mN at low power and 237–238 mN at the wear test full power level in Table 2. Thrust efficiencies were between about 0.49–0.50 at low power to about 0.69–0.70 at the wear test full power level. Specific impulses were 2200–2210 s at low power and

4080–4120 s at the wear test full power level. The specific impulses of all engines at high power point of the throttle table (listed on Table 1) were 4060–4090 s. A beam voltage of 1790 V was required to achieve specific impulses of greater than 4050 s at this full power point.

Table 6 compares the performance test results of all three engines to the performance requirements. As indicated in the table, all three ion engines satisfied the NEXT project performance requirements.

Discharge Losses

Discharge losses were very similar for EM1 and EM2. As Tables 4 and 5 show, discharge losses for EM1 were only 3–6 W/A greater than those for EM2 at beam currents greater than 2.00 A, and 4–13 W/A greater than those for EM2 at beam currents less than or equal to 2.00 A. Discharge losses for LM2 were within 6 W/A of those for EM1 and EM2 at beam currents greater than 2.00 A. However, this disparity grew to 12–32 W/A for beam currents less than or equal to 2.00 A. It is speculated that the differences in discharge losses for LM2 were due to differences in the construction of the discharge chamber.

Discharge losses for all three engines generally decreased with increasing total voltage (i.e. the sum of the absolute values of the beam and accelerator power supply voltages). This is demonstrated in Fig. 4 for LM2 at various beam currents. At the 1.20 A beam current case, discharge losses increased by 16% as the total voltage was decreased from 2050 V to 794 V.

This discharge loss increase with decreasing total voltage is largely due to a decreasing screen grid ion transparency. To remove the effect of screen grid ion transparency, discharge power was plotted as a function total ion current arriving at the screen grid in Fig. 5 at all total voltages tested. Here, the total ion current is equal to the beam current divided by the measured screen grid ion transparency. Screen grid ion transparencies for these tests ranged from 0.81 to 0.94. Figure 5 shows that discharge power monotonically increases with increasing total ion current, as expected.

Ion Optics' Performance

Impingement-limited total voltage is a measure of ion optics' current extraction capability, and, therefore, a measure of ion optics' perveance. Impingement-limited total voltages were determined from plots of accelerator current as a function of total voltage where the slope was –0.02 mA/V (i.e. the NSTAR criterion). Figure 6 shows beam current as a function the impingement-limited total voltage for LM2, EM1, and EM2. Also shown in Fig. 6 is the lowest throttled total voltage for each beam current in Tables 1 and 2. As the figure shows, the ion optics of all three ion engines offer substantial perveance margin (i.e. the difference between the impingement-limited total voltage and the lowest total voltage set point for a given beam current). The lowest perveance margin occurred at the lowest beam current and was about 140 V. Perveance margin is expected to increase as the engine wears due to accelerator grid aperture enlargement from sputter erosion.[12]

The impingement-limited total voltages of EM1 and EM2 were similar and were within about 30 V of each other. The impingement-limited total voltages of LM2 were generally less than those of EM1 or EM2, and this disparity increased with increasing beam current. It is speculated that this difference was due, in part, to a slightly larger cold grid gap for EM1 and EM2, which can lead to higher impingement-limited total voltages. The three ion engines, however, still met all perveance requirements.

The electron backstreaming limit is the highest accelerator voltage that will prevent beam plasma electrons from backstreaming through the ion optics. The electron backstreaming limit was determined by lowering the magnitude of the accelerator grid voltage until the indicated beam current increased by 0.1–1 mA due to backstreaming electrons.

Figure 7a shows the electron backstreaming limit as a function of beam power supply voltage at various beam currents for EM1 and EM2. As Fig. 7a demonstrates, the electron backstreaming limits of EM1 and EM2 were similar, with measured values within 9 V of each other.

Figure 7b shows the electron backstreaming limit as a function of beam power supply voltage at various beam currents for LM2 and EM1. As Fig. 7b demonstrates, the electron backstreaming limits of EM1 were 16–31 V higher than those of LM2. This difference was due to the thicker accelerator grid and slightly larger cold grid gap of EM1. The effect of accelerator thickness on the electron backstreaming limit has been reported in Ref. 7. The minimum electron backstreaming margins (i.e. the difference between the absolute values of the accelerator voltage set point and electron backstreaming limit) were 42 V for LM2 and 60 V for EM1 and EM2. Electron backstreaming margins for the NEXT ion engines were greater than those for the NSTAR ion engine.[12,13]

*Radial Beam Current Density Profile*s

Radial beam current density profiles were used to determine radial current density distributions and peak

current densities for beam flatness parameter calculations. Regarding beam current density measurements, no attempt was made to repel charge-exchange ions from the probe or to account for secondary electron emission due to ion bombardment. Integration of the radial beam current density profiles (assuming azimuthal symmetry) yielded beam currents that were higher than the measured beam current by as much as 8%. Possible sources of error are discussed in Refs. 13 and 14.

Sample radial beam current density distributions are shown in Fig. 8 for EM1. As the figure demonstrates, the shape functions of the ion current density profiles were similar at all beam currents evaluated. The radial profiles were also slightly non-axisymmetric near the center. This asymmetry is an artifact of the engine discharge chamber plasma.[7,13,14]

Ion engine beam flatness parameters (i.e. the ratio of average-to-peak ion current density) for LM2 and EM1 are compared in Fig. 10. Beam flatness parameters of EM1 were 45–85% higher than those of the NSTAR engine reported in Ref. 13 for the same average ion current densities.

The increased beam flatness offered by the NEXT ion engine is significant because of its effects on reducing the magnitude of the electron backstreaming limit, and possibly increasing ion optics perveance and screen grid ion transparencies.[7] The higher beam flatness parameters of the NEXT LM ion engine can also lead to reduced accelerator aperture enlargement near the grid center, and, therefore, increased accelerator grid service life.[7]

Engine Inlet Pressures for EM1

Engine inlet pressure measurements with cold gas flow (i.e. without the engine powered and at room temperature) as a function of propellant flow were made to provide lower limit inlet pressures. Figure 10 shows engine inlet pressure as a function cold gas flow for the main, cathode, and neutralizer propellant lines. During these measurements, the ion engine temperature was between 4–8 °C.

The high inlet pressures of the cathode and main plenum propellant lines in Fig. 10 were due to viscosity effects from the 0.14 mm inner diameter tubing used within the ion engine and propellant isolators. This viscosity effect is further demonstrated by the non-linear relationship between gas flow and inlet pressure for the main plenum and cathode plots. On the other hand, viscosity effects on the neutralizer propellant line were small due largely to the insignificant tubing lengths. As a result, neutralizer inlet pressure was nearly linear with cold gas flow, as would be expected for a choked flow condition at the neutralizer cathode orifice.

Main, cathode, and neutralizer inlet pressure ranges over the throttle table flow range listed in Tables 1 and 2 were 4270–8400 Pa (32–63 Torr), 1730–2130 Pa (13–16 Torr), and 730–990 Pa (5.5–7.4 Torr), respectively.

With these baselines established, the ion engine was operated at various power levels and the inlet pressures monitored as a function of time to determine pressure transients. Figures 11, 12, and 13 show the main, cathode, and neutralizer inlet pressures, respectively, as functions of time from engine startup to steady state. Also plotted on these figures were selected engine temperatures for reference.

As Figs. 11 and 12 show, main plenum and cathode inlet pressures required about 6 hours to increase to steady-state. This long duration of increasing inlet pressure was likely due to the slow heating of the propellant tubing lines within the ion engine. This is demonstrated by the temperature profiles in Figs. 11 and 12. In Fig. 11, for example, discharge chamber components such as the front magnet ring and the chamber support achieved steady-state temperatures within 4 hours due to the close proximity of these components to the heat source (i.e. the discharge). The socket, however, was located further from the heat source and, therefore, required > 5 hours to achieve steady-state.

As Fig. 13 shows, however, the neutralizer inlet pressure only required about 0.5 hour to reach steady-state. This indicates that neutralizer temperatures likely reached steady-state within this time frame as well.

Steady-state inlet pressures for the main, cathode, and neutralizer propellant lines are listed in Table 7. Maximum main, cathode, and neutralizer pressures were 12,000 Pa (90.2 Torr), 3110 Pa (23.3 Torr), and 8540 Pa, (64.1 Torr), respectively, at the full power point of the NEXT throttle table.

Because the NEXT propellant management system utilizes non-choked flow restrictors, the high engine inlet pressures of the propellant lines will need to be considered in the propellant management system design to maintain the tight flow tolerance requirement.

Engine Operating Temperatures for EM1

Ion engine temperatures at beam currents of 1.20 A and 3.52 A as a function of time from engine startup are shown in Figs. 14 and 15, respectively. At the 1.20 A beam current case, the engine was operated at the highest and lowest beam power supply voltages (i.e. 1800 V and 679 V, respectively), and, therefore, the highest and lowest total voltages. The highest beam power supply voltage at 1.20 A resulted in the lowest measured steady-state temperatures because this high total voltage required the lowest discharge power (as discussed in a prior section). However, this temperature difference was small, with changes of ≤ 7 C°.

As Figs. 14 and 15 indicate, magnet ring, chamber support, and ion optics mounting ring temperatures at low and full power required about 3–4 hours to reach steady-state. The socket temperature, however, required about 5 hours to reach steady-state, likely due to its longer distance from the discharge chamber.

Steady-state engine operating temperatures ranges were 179–303 °C for the discharge chamber magnet rings, 132–213 °C for the ion optics mounting ring, and 97–159 °C for the socket. Peak magnet ring temperatures were greater than 100 C° below the magnet stabilization temperature. The steady-state temperature ranges, as well as the temperature transient behavior in Figs. 14 and 15, are provided to verify thermal models for the NEXT ion engine.

Conclusions

The performance test results of three NEXT ion engines, labeled LM2, EM1, and EM2, were presented.

The ion engines exhibited peak specific impulse and thrust efficiency ranges of 4060–4090 s and 0.68–0.69, respectively, at the full power point of the NEXT throttling table. The performance of these ion engines satisfied all NEXT project performance requirements.

The ion optics of all three engines provided a minimum perveance margin of 140 V and a minimum electron backstreaming margin of 42 V. Beam flatness parameters were significantly improved over the NSTAR ion engine, which is expected to improve accelerator grid service life.

The results of engine inlet pressure and temperature measurements were presented for engine EM1. Maximum main, cathode, and neutralizer pressures were 12,000 Pa (90.2 Torr), 3110 Pa (23.3 Torr), and 8540 Pa, (64.1 Torr), respectively, at the full power point of the NEXT throttle table. Main plenum and cathode inlet pressures required about 6 hours to increase to steady-state, while the neutralizer required only about 0.5 hour. The pressure measurements will be used to define the design of the NEXT propellant management system.

Steady-state engine operating temperatures ranges were 179–303 °C for the discharge chamber magnet rings, 132–213 °C for the ion optics mounting ring, and 97–159 °C for the socket. These steady-state temperature ranges, as well as the temperature transient behavior are provided to verify thermal models for the NEXT ion engine.

References

[1] Polk, J.E., et al., "In-Flight Performance of the NSTAR Ion Propulsion System on the Deep Space One Mission," IEEE Aerospace Conference Paper 8.0304, March 2000.

[2] Patterson, M.J., et al., "NEXT: NASA's Evolutionary Xenon Thruster Development Status," AIAA Paper 2003-4862, July 2003.

[3] Patterson, M.J., et al., "NEXT: NASA's Evolutionary Xenon Thruster," AIAA Paper 2002-3832, July 2002.

[4] Christensen, J.A., et al., "Design and Fabrication of a Flight Model 2.3 kW Ion Thruster for the Deep Space 1 Mission," AIAA Paper 98-3327, July 1998.

[5] Patterson, M.J., et al., "Space Station Cathode Design, Performance, and Operating Specifications," IEPC Paper 97-170, August 1997.

[6] Kovaleski, S.K., et al., "A Review of Testing of Hollow Cathodes for the International Space Station Plasma Contactor," IEPC Paper 01-271, October 2001.

[7] Soulas, G.C., Patterson, M.J., and Haag, T.W., "Performance Evaluation of 40 cm Ion Optics for the NEXT Ion Engine," AIAA Paper 2002-3834, July 2002.

[8] Pinero, L.R., Patterson, M.J., and Satterwhite, V.E., "Power Console Development for NASA's Electric Propulsion Outreach Program," IEPC Paper 93-250, September 1993.

[9] Soulas, G.C., et al., "Status of the NEXT Ion Engine Wear Test," AIAA Paper 2003-4863, July 2003.

[10] Patterson, M.J., Haag, T.W., and Hovan, S.A., "Performance of the NASA 30 cm Ion Thruster," IEPC Paper 93-108, September 1993.

[11] Sovey, J.S., "Improved Ion Containment Using a Ring-Cusp Ion Thruster," Journal of Spacecraft and Rockets, vol. 21, no. 5, September-October 1984, p. 489.

[12] Polk, et al., "An Overview of the Results from an 8200 Hour Wear Test of the NSTAR Ion Thruster," AIAA Paper 99-2446, June 1999.
[13] Soulas, G.C., "Performance Evaluation of Titanium Ion Optics for the NASA 30 cm Ion Thruster," IEPC Paper 01-092, October 2001.
[14] Soulas, G.C., "Performance of Titanium Optics on a NASA 30 cm Ion Thruster," AIAA Paper 2000-3814, July 2000.

Table 1.—NEXT ion engine throttle table.

Anticipated Engine Input Power,[a] kW	Beam Current, A	Beam P.S. Voltage,[b] V	Accelerator Voltage, V	Main Plenum Flow Rate,[c] sccm	Discharge Cathode Flow Rate,[c] sccm	Neutalizer Flow Rate,[d] sccm	Neutralizer Keeper Current, A
1.07	1.20	680	–115	15.7	3.57	4.01	3.0
1.28	1.20	850	–125	15.7	3.57	4.01	3.0
1.49	1.20	1020	–175	15.7	3.57	4.01	3.0
1.68	1.20	1180	–200	15.7	3.57	4.01	3.0
1.94	1.20	1400	–220	15.7	3.57	4.01	3.0
2.14	1.20	1570	–235	15.7	3.57	4.01	3.0
2.42	1.20	1800	–250	15.7	3.57	4.01	3.0
2.40	2.00	1020	–175	27.1	3.87	4.41	3.0
2.71	2.00	1180	–200	27.1	3.87	4.41	3.0
3.15	2.00	1400	–220	27.1	3.87	4.41	3.0
3.49	2.00	1570	–235	27.1	3.87	4.41	3.0
3.96	2.00	1800	–250	27.1	3.87	4.41	3.0
3.18	2.70	1020	–175	37.6	4.26	4.75	3.0
3.61	2.70	1180	–200	37.6	4.26	4.75	3.0
4.20	2.70	1400	–220	37.6	4.26	4.75	3.0
4.66	2.70	1570	–235	37.6	4.26	4.75	3.0
5.30	2.70	1800	–250	37.6	4.26	4.75	3.0
4.12	3.10	1180	–200	43.5	4.54	4.95	3.0
4.80	3.10	1400	–220	43.5	4.54	4.95	3.0
5.33	3.10	1570	–235	43.5	4.54	4.95	3.0
6.06	3.10	1800	–250	43.5	4.54	4.95	3.0

[a]Nominal values.
[b]Power supply voltage.
[c]Main-to-discharge cathode flow split selected to result in a 23.5–27 V discharge voltage.
[d]Neutralizer flow with beam extraction; without beam extraction and for ignition, flow is set to 6.00 sccm.

Table 2.—NEXT ion engine high beam current and wear test operating points.

Anticipated Engine Input Power,[a] kW	Beam Current, A	Beam P.S. Voltage,[b] V	Accelerator Voltage, V	Main Plenum Flow Rate,[c] sccm	Discharge Cathode Flow Rate,[c] sccm	Neutalizer Flow Rate,[d] sccm	Neutralizer Keeper Current, A
4.66	3.52	1180	–200	49.6	4.87	5.16	3.0
5.42	3.52	1400	–220	49.6	4.87	5.16	3.0
6.03	3.52	1570	–235	49.6	4.87	5.16	3.0
6.85[e]	3.52[e]	1800[e]	–250/–210[e]	49.6[e]	4.87[e]	5.16[e]	3.0[e]

[a]Nominal values.
[b]Power supply voltage.
[c]Main-to-discharge cathode flow split selected to result in a 23.5–27 V discharge voltage.
[d]Neutralizer flow with beam extraction; without beam extraction and for ignition, flow is set to 6.00 sccm.
[e]Wear test operating point.

Table 3.—NEXT engine LM2 performance test results in VF6.

Beam Current, A	Beam Voltage, V	Thruster Input Power, kW	Discharge Losses, W/A	Thrust Efficiency	Thrust,[a] mN	Specific Impulse, s
1.203	671	1.12	215	0.485	49.9	2210
1.202	841	1.31	205	0.517	55.8	2470
1.206	1010	1.51	198	0.543	61.4	2720
1.203	1170	1.69	192	0.558	65.9	2920
1.205	1390	1.95	189	0.574	71.8	3180
1.205	1560	2.16	187	0.583	76.1	3370
1.203	1790	2.43	185	0.592	81.4	3610
2.004	1010	2.43	172	0.609	102	2970
2.004	1170	2.74	169	0.624	110	3190
2.010	1390	3.18	165	0.641	120	3480
2.009	1560	3.52	164	0.649	127	3690
2.005	1790	3.98	163	0.657	135	3950
2.708	1010	3.22	152	0.638	138	3050
2.707	1170	3.64	148	0.653	149	3280
2.702	1390	4.21	144	0.666	161	3560
2.706	1560	4.68	142	0.675	170	3780
2.710	1790	5.32	141	0.684	183	4050
3.102	1170	4.14	141	0.662	169	3300
3.106	1390	4.81	137	0.677	185	3600
3.102	1560	5.33	134	0.684	195	3810
3.106	1790	6.06	132	0.693	210	4090
3.520[b]	1170[b]	4.68[b]	136[b]	0.670[b]	192[b]	3330[b]
3.521[b]	1390[b]	5.44[b]	133[b]	0.684[b]	209[b]	3620[b]
3.531[b]	1560[b]	6.06[b]	131[b]	0.693[b]	222[b]	3850[b]
3.524[b]	1790[b]	6.86[b]	130[b]	0.700[b]	238[b]	4120[b]

[a]Thrust correction factor due to beam divergence assumed to be about 0.98; ratio of doubly-to-singly-charge ion current assumed to be 0.034—0.044.
[b]Not a throttle table operating point.

Table 4.—NEXT engine EM1 performance test results in VF6.

Beam Current, A	Beam Voltage, V	Thruster Input Power, kW	Discharge Losses, W/A	Thrust Efficiency	Thrust,[a] mN	Specific Impulse, s
1.201	670	1.08	190	0.495	49.6	2210
1.204	841	1.28	184	0.526	55.7	2480
1.202	1010	1.48	177	0.548	61.1	2710
1.204	1170	1.67	173	0.564	65.7	2920
1.202	1390	1.92	167	0.579	71.4	3180
1.203	1560	2.13	164	0.588	75.7	3370
1.203	1790	2.41	163	0.597	81.2	3610
2.002	1170	2.72	160	0.624	109	3180
2.005	1790	3.95	148	0.658	135	3930
2.703	1170	3.63	147	0.649	147	3260
2.705	1790	5.29	135	0.682	182	4040
3.098	1170	4.14	143	0.660	169	3300
3.101	1790	6.04	131	0.689	209	4070
3.518[b]	1170[b]	4.70[b]	143[b]	0.663[b]	192[b]	3320[b]
3.517[b]	1390[b]	5.44[b]	137[b]	0.677[b]	208[b]	3610[b]
3.521[b]	1560[b]	6.05[b]	133[b]	0.687[b]	221[b]	3830[b]
3.521[b]	1790[b]	6.85[b]	129[b]	0.696[b]	237[b]	4100[b]

[a]Thrust correction factor due to beam divergence assumed to be about 0.98; ratio of doubly-to-singly-charge ion current assumed to be 0.034–0.044.
[b]Not a throttle table operating point.

Table 5.—NEXT engine EM2 performance test results in VF11.

Beam Current, A	Beam Voltage, V	Thruster Input Power, kW	Discharge Losses, W/A	Thrust Efficiency	Thrust,[a] mN	Specific Impulse, s
1.203	670	1.08	183	0.496	49.7	2200
1.200	841	1.28	177	0.525	55.5	2460
1.202	1010	1.48	173	0.547	61.0	2710
1.201	1170	1.67	169	0.560	65.6	2900
1.199	1390	1.91	161	0.575	71.3	3150
1.201	1560	2.12	159	0.585	75.6	3350
1.201	1790	2.40	157	0.592	81.0	3580
1.998	1170	2.70	147	0.626	109	3170
2.001	1790	3.94	137	0.655	135	3910
2.698	1170	3.63	142	0.646	147	3250
2.702	1790	5.29	132	0.678	182	4020
3.101	1170	4.16	137	0.651	169	3270
3.101	1790	6.08	125	0.684	209	4060
3.519[b]	1170[b]	4.70[b]	138[b]	0.660[b]	192[b]	3310[b]
3.515[b]	1350[b]	5.31[b]	133[b]	0.672[b]	205[b]	3540[b]
3.518[b]	1560[b]	6.05[b]	128[b]	0.682[b]	221[b]	3810[b]
3.518[b]	1790[b]	6.86[b]	124[b]	0.690[b]	237[b]	4080[b]

[a]Thrust correction factor due to beam divergence assumed to be about 0.98; ratio of doubly-to-singly-charge ion current assumed to be 0.034–0.044.
[b]Not a throttle table operating point.

Table 6.—NEXT ion engine performance requirements and test results for LM2, EM1, and EM2.

Performance Requirements	LM2 Test Results	EM1 Test Results	EM2 Test Results
Specific impulse ≥ 4050 s	4090 s	4070 s	4060 s
Low power thrust efficiency > 0.42	0.49	0.50	0.50
High power thrust efficiency > 0.63	0.69	0.69	0.68

Table 7.—NEXT engine EM1 propellant inlet pressures in VF11.

Operating Condition[a]	Xenon Flow Rate, sccm			Pressure, Pa (Torr)		
	Main Plenum	Cathode	Neutralizer	Main Plenum	Cathode	Neutralizer
J_b = 3.52 A,[b] V_{b-PS} = 1800 V[b]	49.6	4.87	5.16	13,300 (99.9)	3280 (24.6)	7850 (58.9)
			6.00			8980 (67.4)
J_b = 3.10 A, V_{b-PS} = 1180 V	43.5	4.54	4.95	12,000 (90.2)	3110 (23.3)	7260 (54.5)
			6.00			8540 (64.1)
J_b = 1.20 A, V_{b-PS} = 1800 V	15.7	3.57	4.01	5910 (44.3)	2400 (18.0)	4640 (34.8)
J_b = 1.20 A, V_{b-PS} = 679 V	15.7	3.57	4.01	5970 (44.8)	2420 (18.2)	4640 (34.8)
			6.00			6670 (50.0)
Neutralizer On; J_b = 0			6.00			5470 (41.0)

[a]J_b ≡ beam current and V_{b-PS} ≡ beam power supply voltage.
[b]Not a throttle table operating point.

Figure 1.—NEXT laboratory model engine LM2 with 40 cm beam extraction diameter.

Figure 2.—NEXT engineering model engine EM1 instrumented with pressure taps for propellant line pressure measurements at the engine inlet.

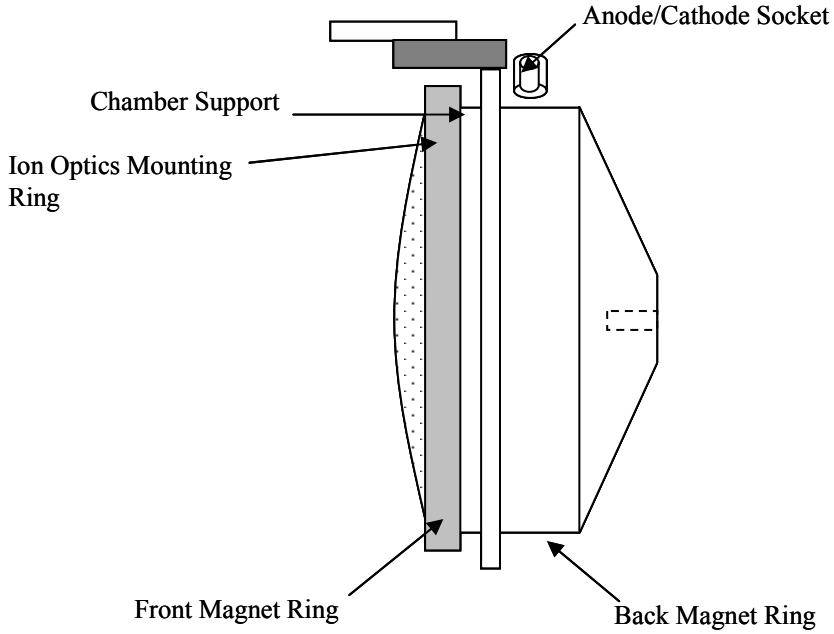

Figure 3.—Locations of thermocouples on a side view of NEXT engine EM1 with plasma screen and front mask removed from drawing for clarity. (Drawing not to scale.)

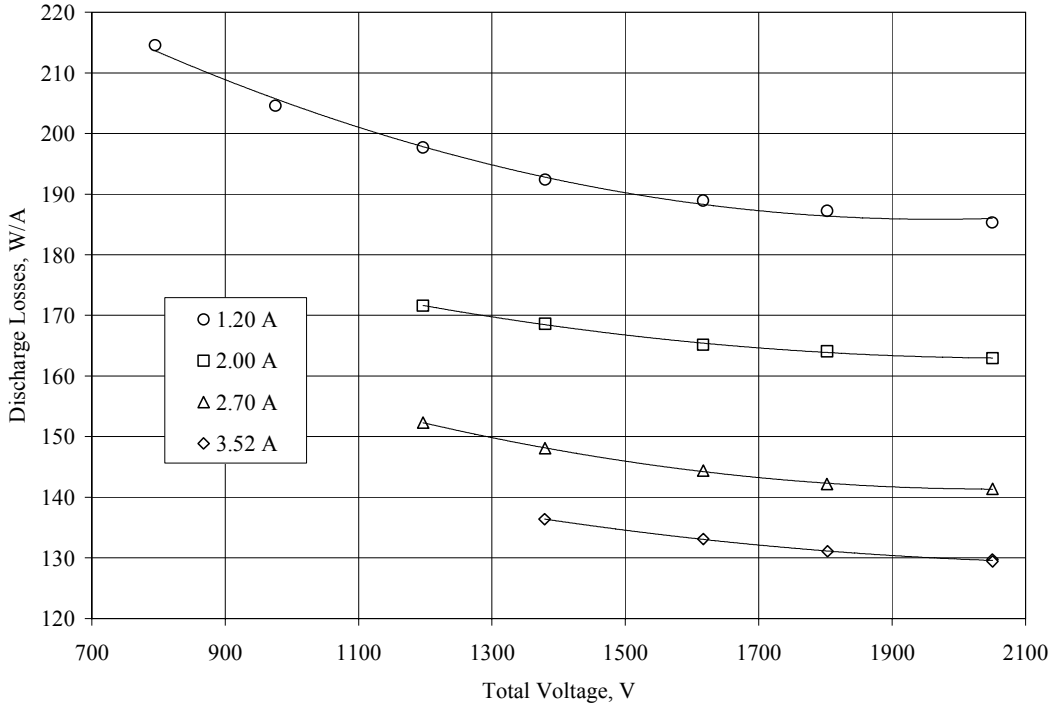

Figure 4.—Discharge losses as a function of total voltage for LM2 at various beam currents.

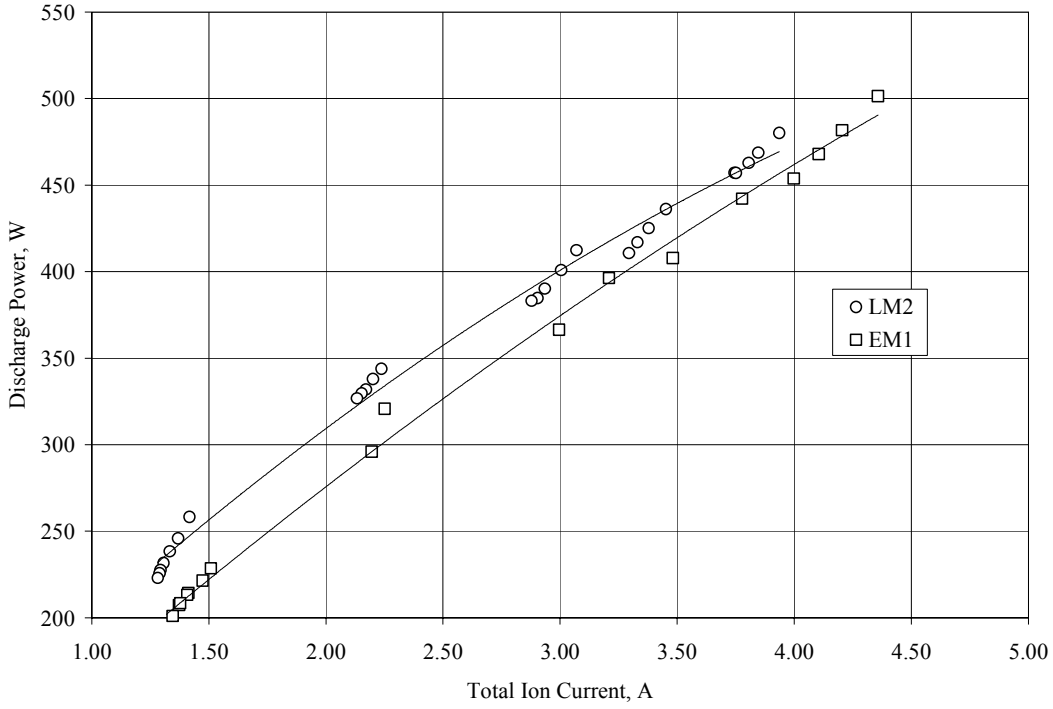

Figure 5.—Discharge power as a function of total ion current to the screen grid at various total voltages for LM2 and EM1.

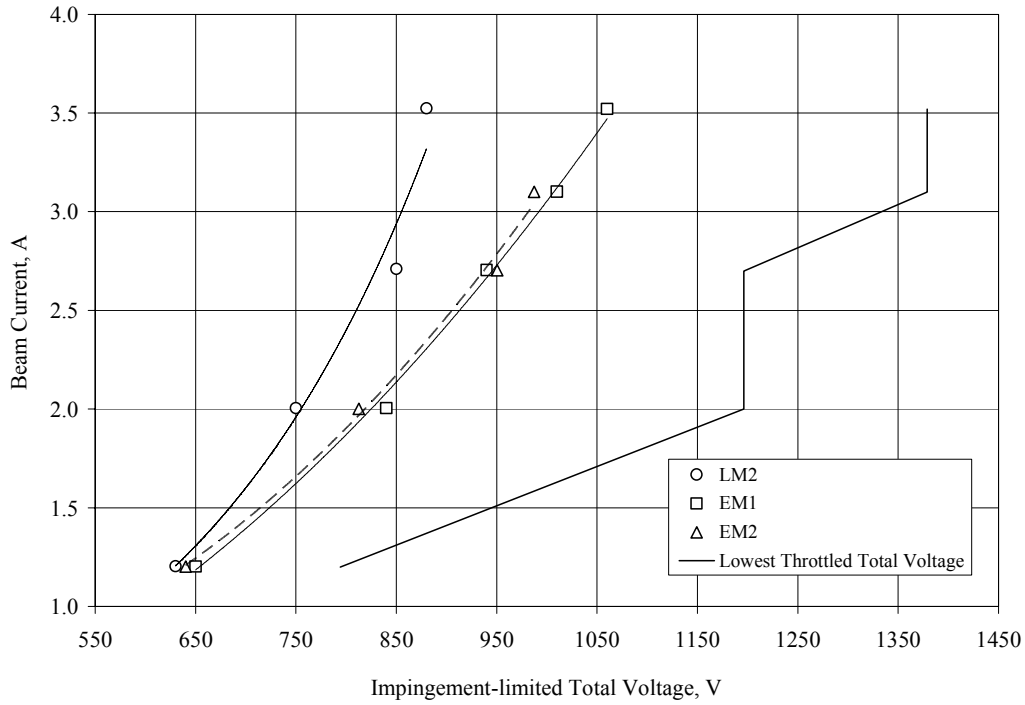

Figure 6.—Beam current as a function of impingement-limited total voltage for LM2, EM1, and EM2.

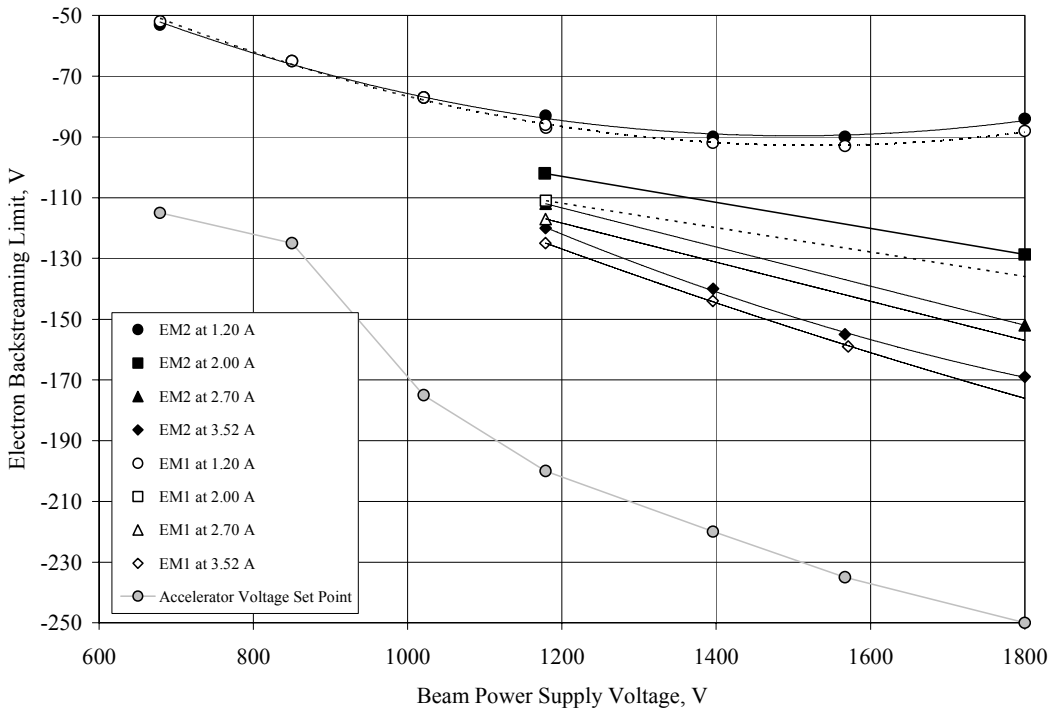

a. Ion engines EM1 and EM2.

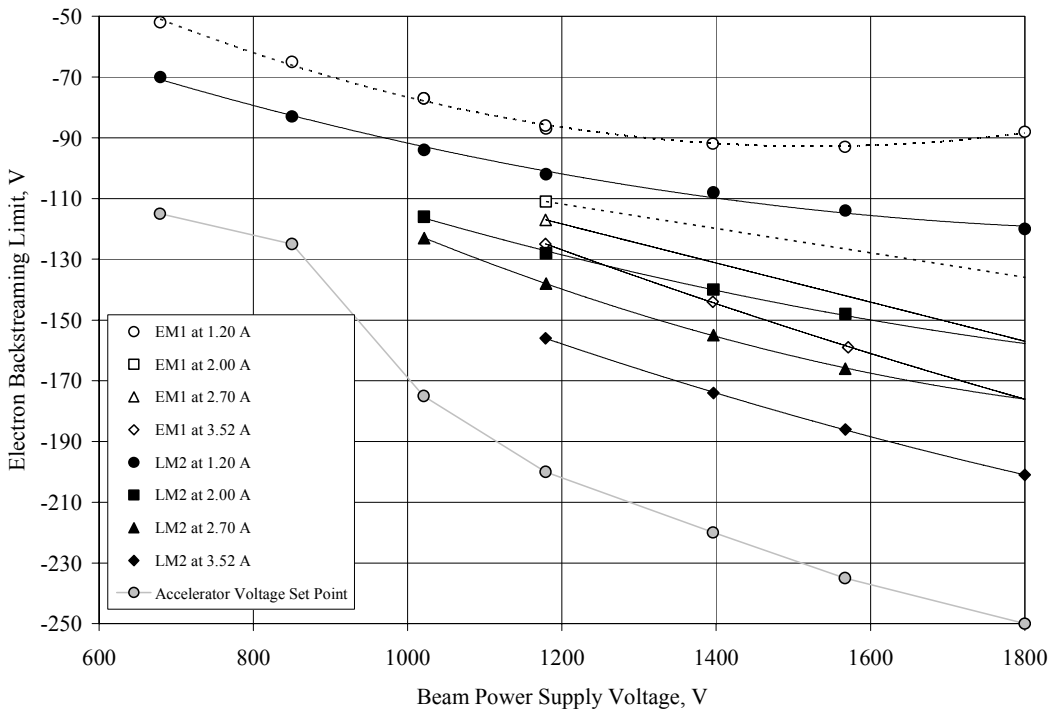

b. Ion engines EM1 and LM2.

Figure 7.—Electron backstreaming limit as a function of beam power supply voltage at various beam currents.

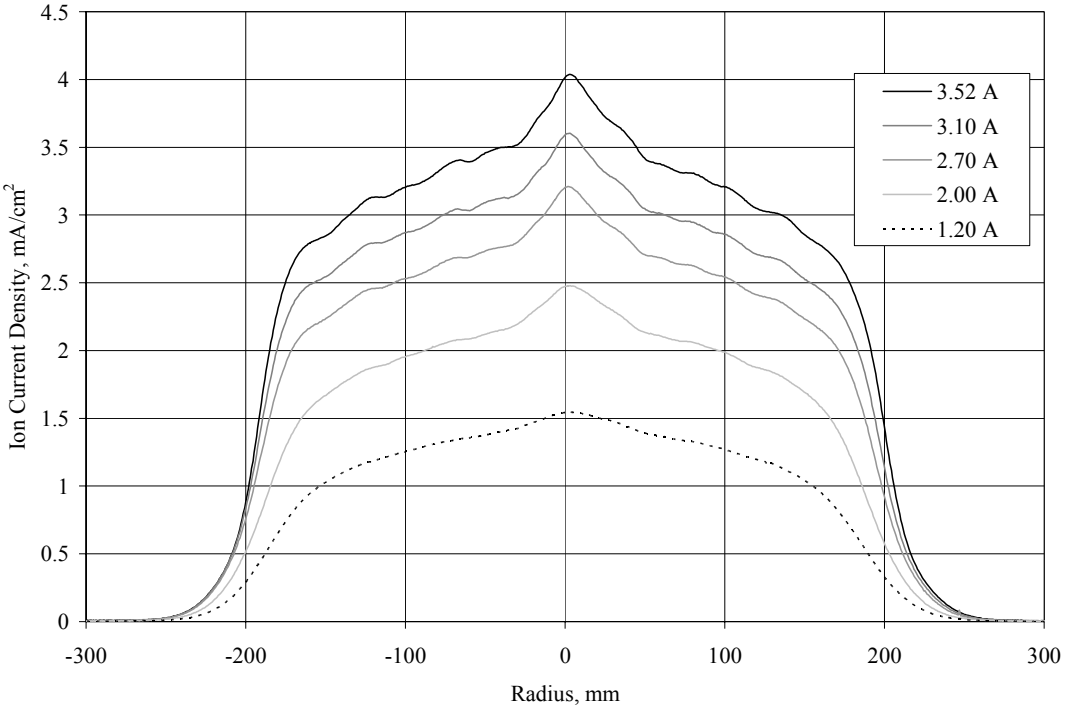

Figure 8.—Sample radial beam current density profiles for EM1 at various beam currents for a beam power supply voltage of 1180 V.

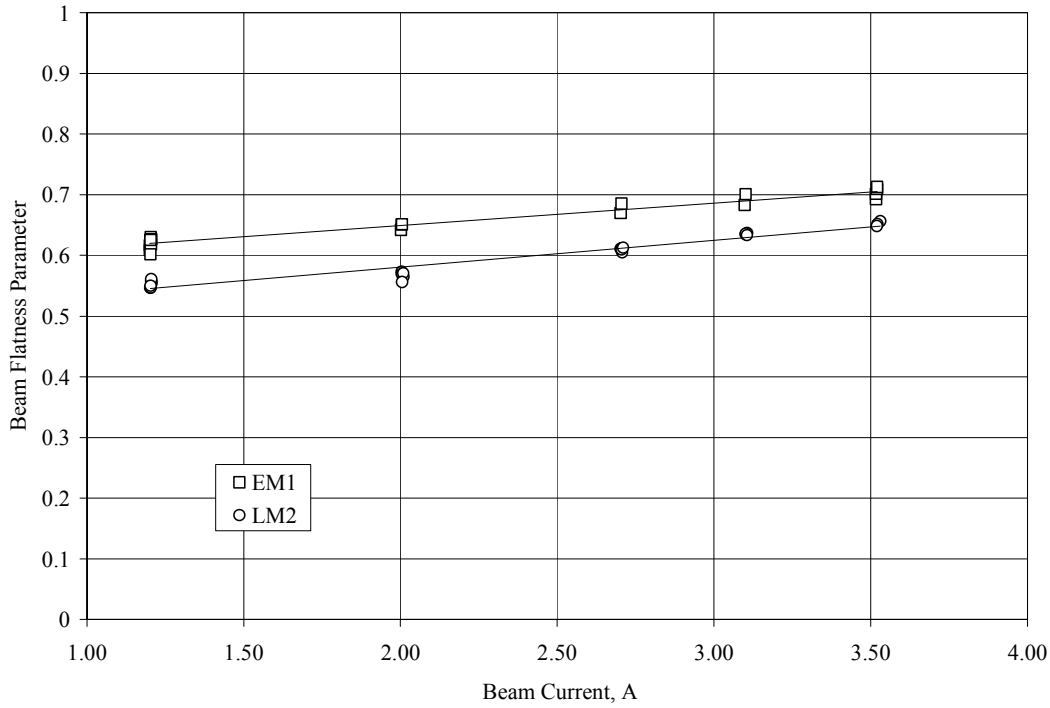

Figure 9.—Beam flatness parameter as a function of beam current for EM1 and LM2.

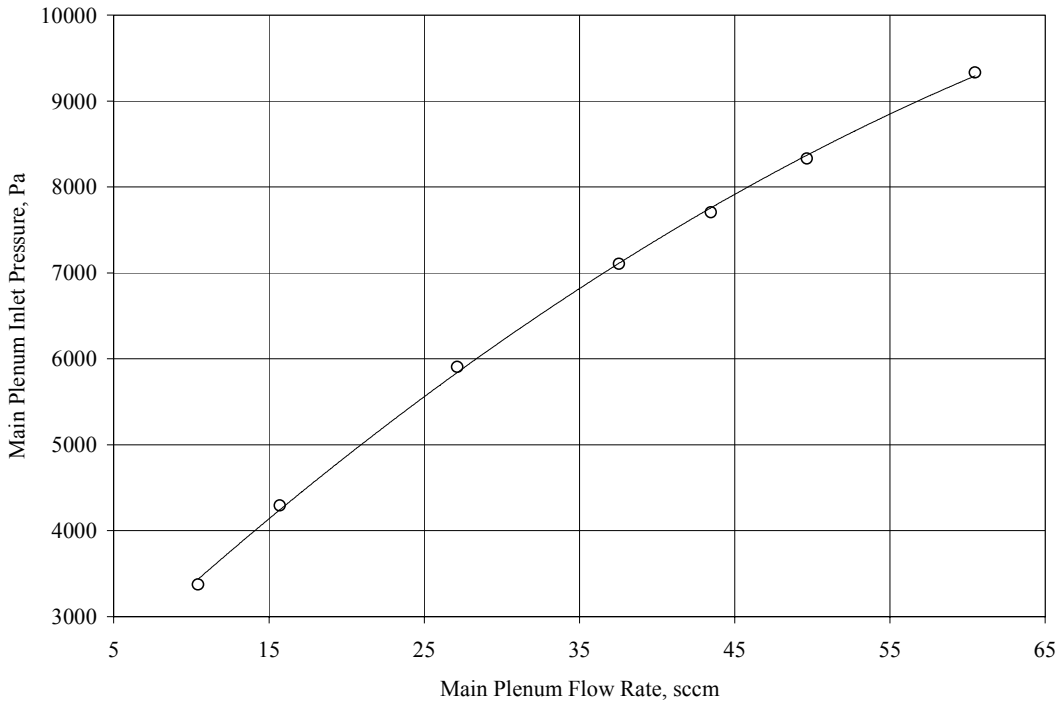

a. Main plenum.

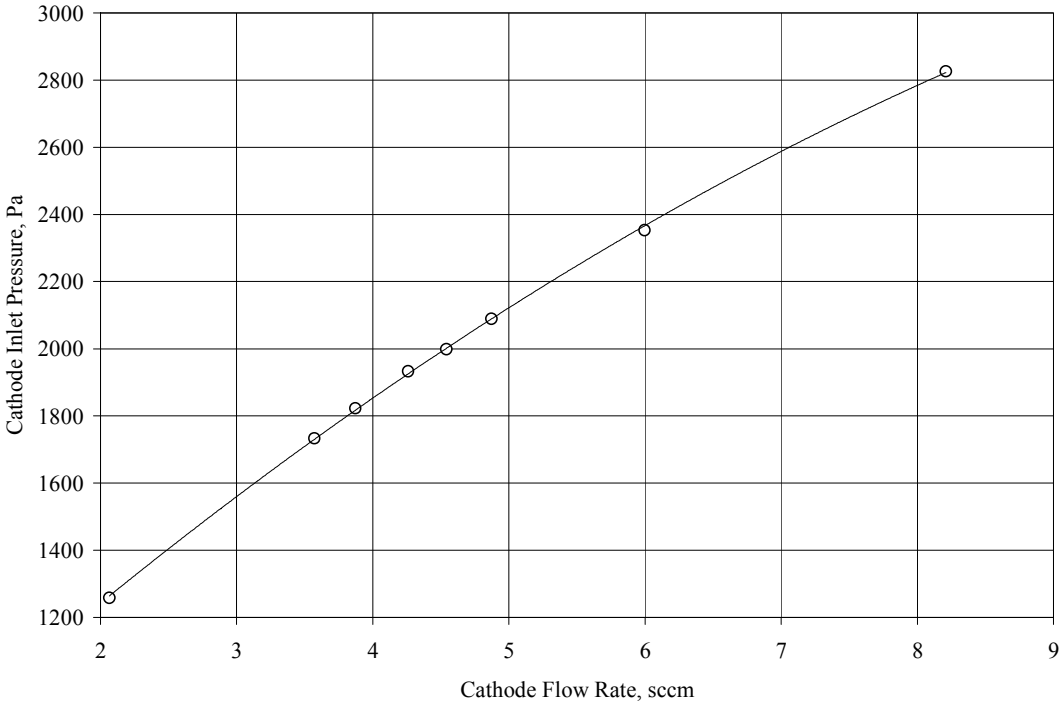

b. Discharge cathode.

Figure 10.—NEXT engine EM1 main, cathode, and neutralizer propellant inlet pressures over a range of cold gas flows (continued).

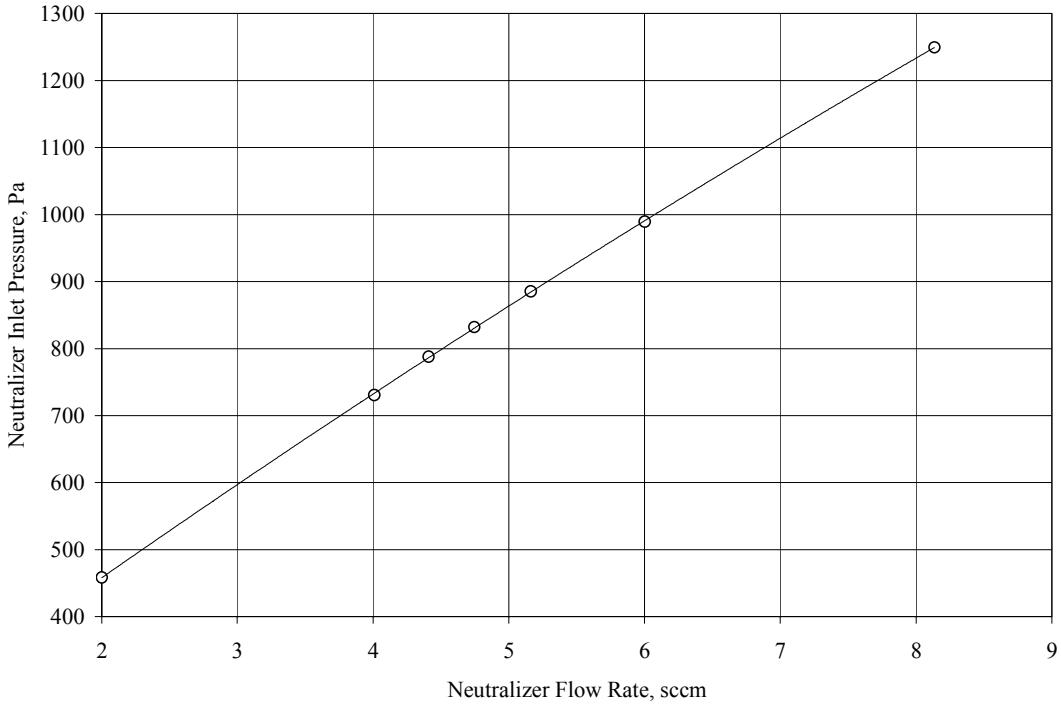

c. Neutralizer.

Figure 10.—NEXT engine EM1 main, cathode, and neutralizer propellant inlet pressures over a range of cold gas flows (concluded).

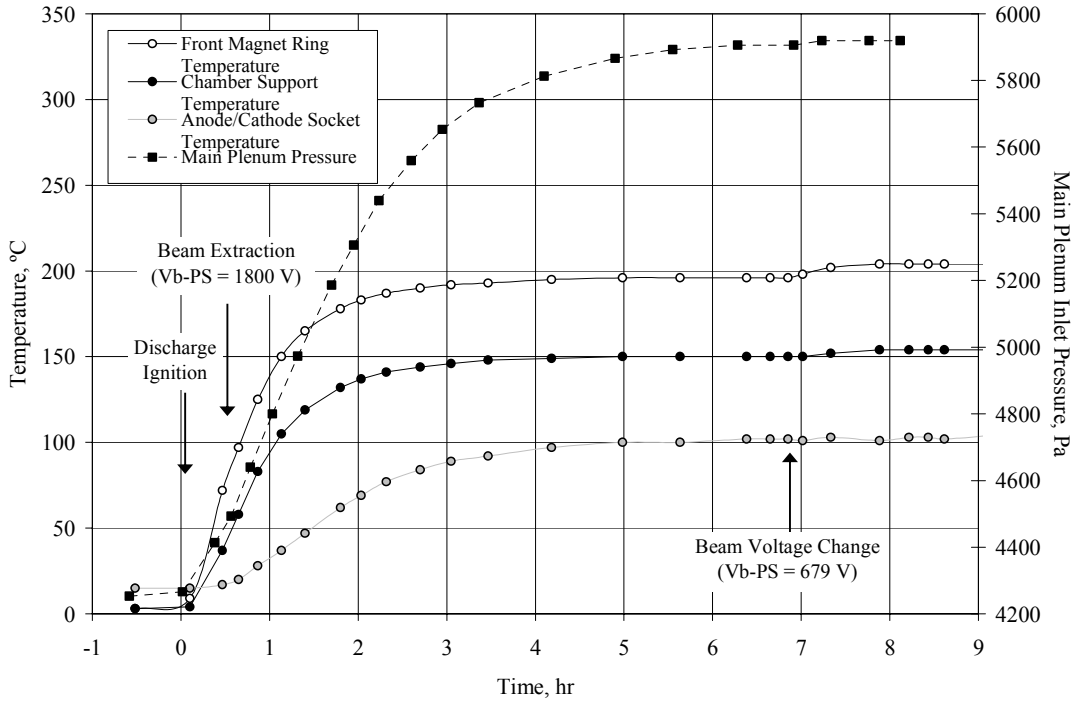

Figure 11.—NEXT engine EM1 main plenum inlet pressure and temperatures at a 1.20 A beam current and 1800 V and 679 V beam power supply voltages. Arrows indicate when discharge ignition, beam extraction, and beam power supply voltage changes occurred.

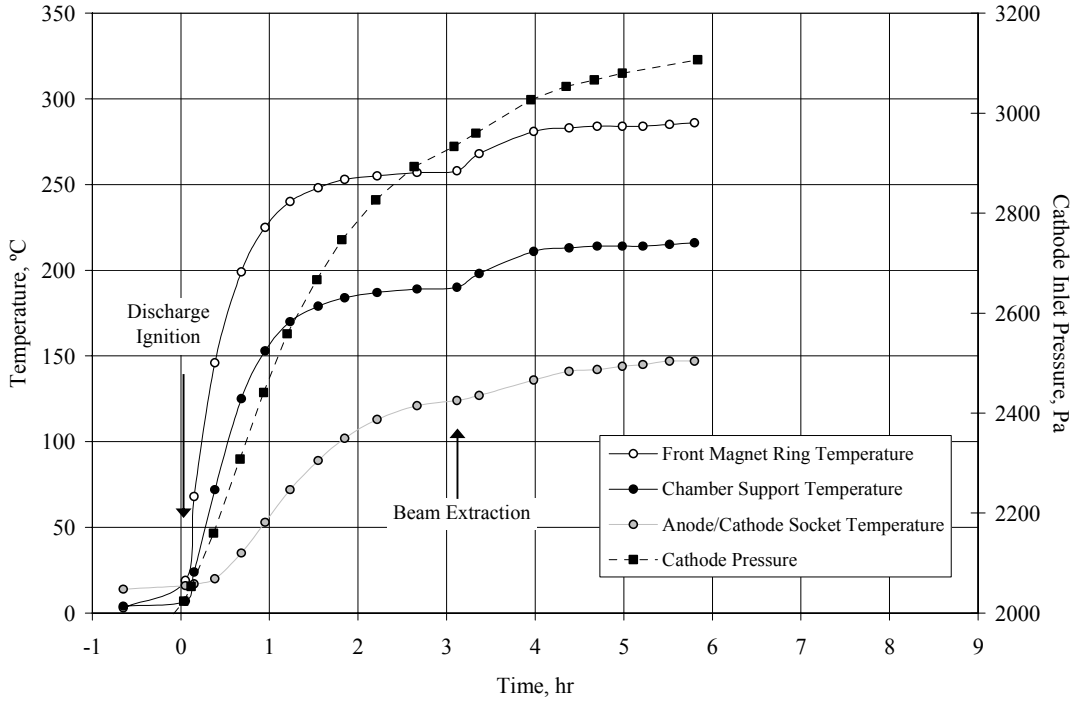

Figure 12.—NEXT engine EM1 cathode inlet pressure and temperatures at a 3.10 A beam current and a 1179 V beam power supply voltage. Arrows indicate when discharge ignition and beam extraction occurred.

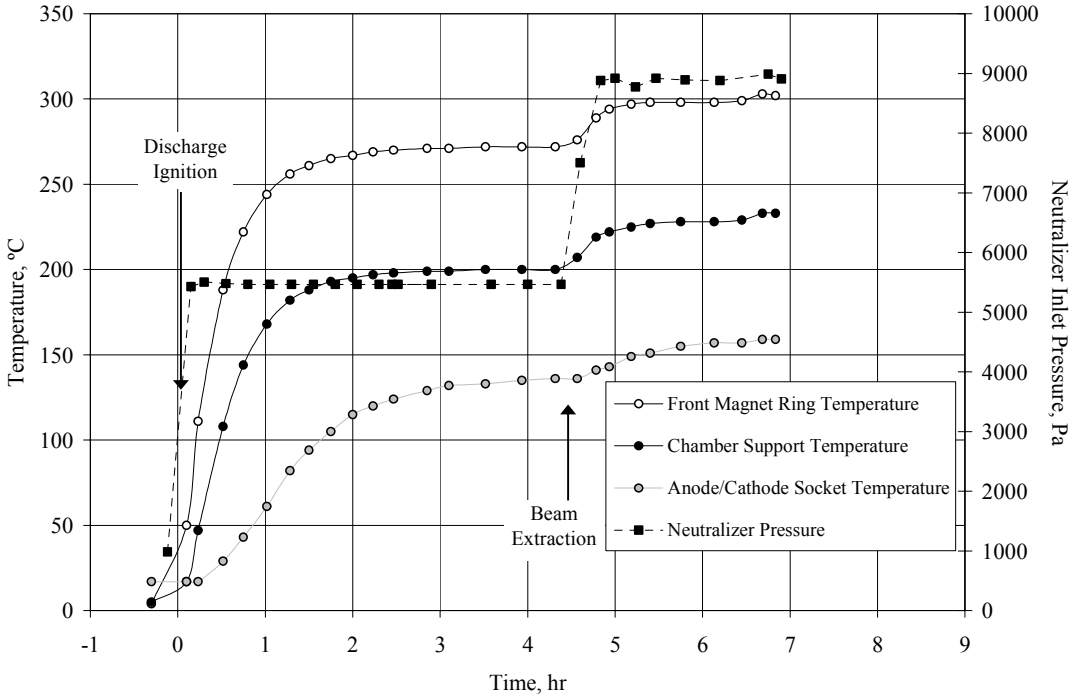

Figure 13.—NEXT engine EM1 neutralizer inlet pressure and temperatures at a 3.52 A beam current and a 1800 V beam power supply voltage. Arrows indicate when discharge ignition and beam extraction occurred.

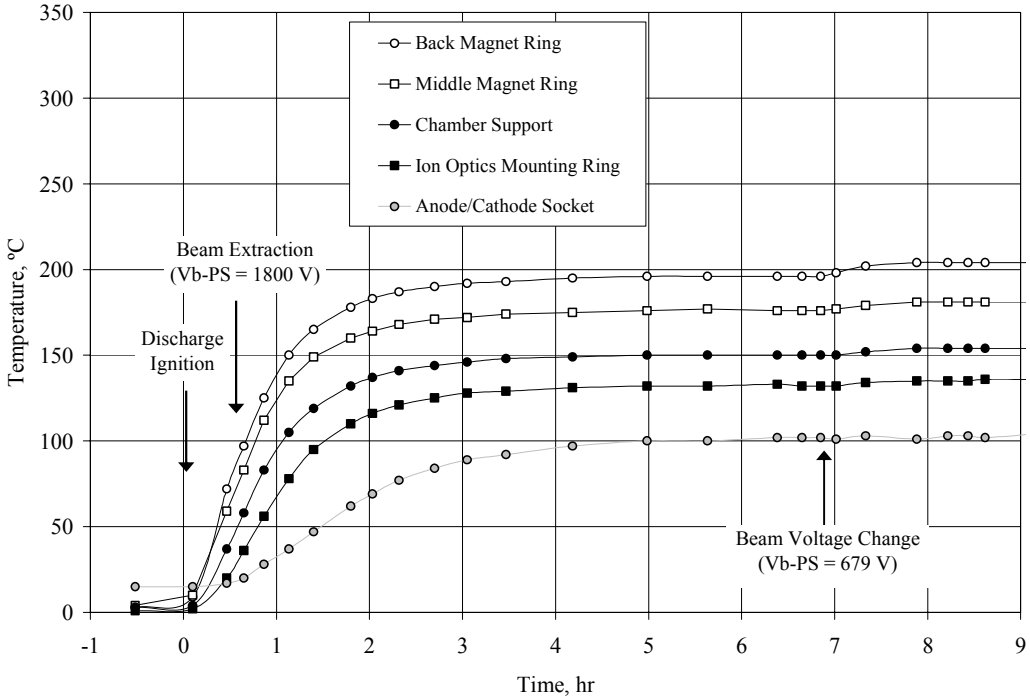

Figure 14.—NEXT engine EM1 temperatures at a 1.20 A beam current and 1800 V and 679 V beam power supply voltages. Arrows indicate when discharge ignition, beam extraction, and beam power supply voltage changes occurred.

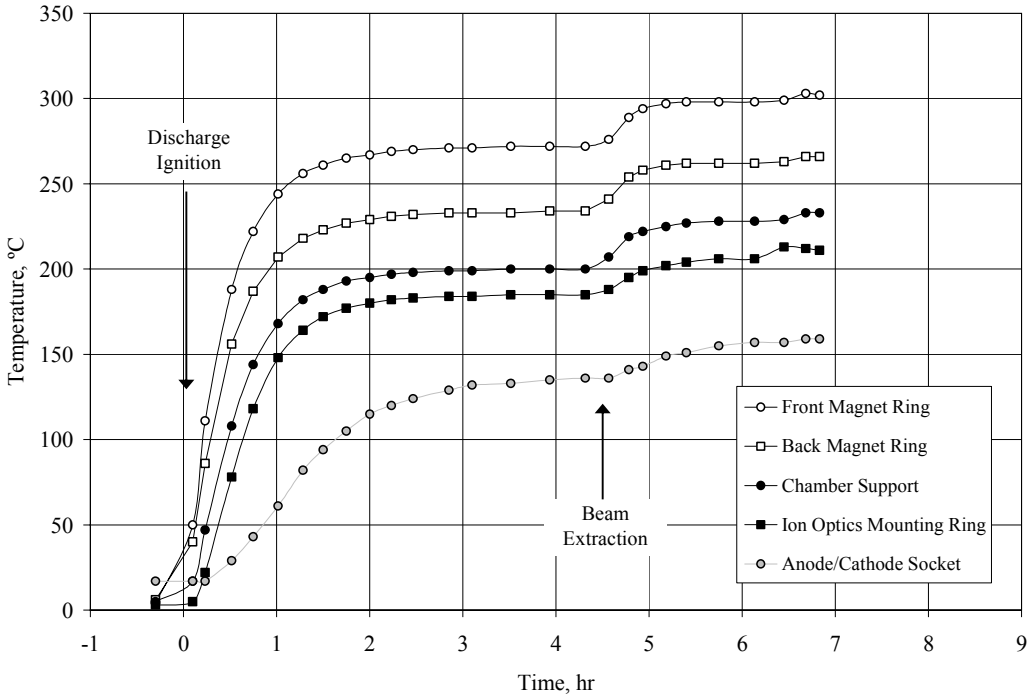

Figure 15.—NEXT engine EM1 temperatures at a 3.52 A beam current and a 1800 V beam power supply voltage. Arrows indicate when discharge ignition and beam extraction occurred.

REPORT DOCUMENTATION PAGE

Form Approved
OMB No. 0704-0188

Public reporting burden for this collection of information is estimated to average 1 hour per response, including the time for reviewing instructions, searching existing data sources, gathering and maintaining the data needed, and completing and reviewing the collection of information. Send comments regarding this burden estimate or any other aspect of this collection of information, including suggestions for reducing this burden, to Washington Headquarters Services, Directorate for Information Operations and Reports, 1215 Jefferson Davis Highway, Suite 1204, Arlington, VA 22202-4302, and to the Office of Management and Budget, Paperwork Reduction Project (0704-0188), Washington, DC 20503.

1. AGENCY USE ONLY (*Leave blank*)

2. REPORT DATE
October 2003

3. REPORT TYPE AND DATES COVERED
Technical Memorandum

4. TITLE AND SUBTITLE
Performance Evaluation of the NEXT Ion Engine

5. FUNDING NUMBERS
WBS–22–800–50–01

6. AUTHOR(S)
George C. Soulas, Matthew T. Domonkos, and Michael J. Patterson

7. PERFORMING ORGANIZATION NAME(S) AND ADDRESS(ES)
National Aeronautics and Space Administration
John H. Glenn Research Center at Lewis Field
Cleveland, Ohio 44135–3191

8. PERFORMING ORGANIZATION REPORT NUMBER
E–14117

9. SPONSORING/MONITORING AGENCY NAME(S) AND ADDRESS(ES)
National Aeronautics and Space Administration
Washington, DC 20546–0001

10. SPONSORING/MONITORING AGENCY REPORT NUMBER
NASA TM—2003-212551
AIAA–2003–5278

11. SUPPLEMENTARY NOTES
Prepared for the 39th Joint Propulsion Conference and Exhibit cosponsored by the AIAA, ASME, SAE, and ASEE, Huntsville, Alabama, July 20–23, 2003. Responsible person, George C. Soulas, organization code 5430, 216–977–7481.

12a. DISTRIBUTION/AVAILABILITY STATEMENT
Unclassified - Unlimited
Subject Category: 20 Distribution: Nonstandard
Available electronically at http://gltrs.grc.nasa.gov
This publication is available from the NASA Center for AeroSpace Information, 301–621–0390.

12b. DISTRIBUTION CODE

13. ABSTRACT ***(Maximum 200 words)***

The performance test results of three NEXT ion engines are presented. These ion engines exhibited peak specific impulse and thrust efficiency ranges of 4060 to 4090 s and 0.68 to 0.69, respectively, at the full power point of the NEXT throttle table. The performance of the ion engines satisfied all project requirements. Beam flatness parameters were significantly improved over the NSTAR ion engine, which is expected to improve accelerator grid service life. The results of engine inlet pressure and temperature measurements are also presented. Maximum main plenum, cathode, and neutralizer pressures were 12,000, 3110, and 8540 Pa, respectively, at the full power point of the NEXT throttle table. Main plenum and cathode inlet pressures required about 6 hours to increase to steady-state, while the neutralizer required only about 0.5 hour. Steady-state engine operating temperature ranges throughout the power throttling range examined were 179 to 303 °C for the discharge chamber magnet rings and 132 to 213 °C for the ion optics mounting ring.

14. SUBJECT TERMS
Ion thruster; Ion engine; Ion propulsion

15. NUMBER OF PAGES
25

16. PRICE CODE

17. SECURITY CLASSIFICATION OF REPORT	18. SECURITY CLASSIFICATION OF THIS PAGE	19. SECURITY CLASSIFICATION OF ABSTRACT	20. LIMITATION OF ABSTRACT
Unclassified	Unclassified	Unclassified	